DOI: 10.1002/ejoc.200900264

A DFT Model Study of the Carbocations Formed via the Fjord- and Bay-Region Diol Epoxide Metabolites of Isomeric Dibenzopyrenes and Naphthopyrene

Gabriela L. Borosky*[a] and Kenneth K. Laali*[b]

Keywords: Hydrocarbons / Polycycles / Carbocations / Density functional calculations / Structure–activity relationships / Polycyclic aromatic hydrocarbons (PAH) / DNA

A density-functional theory (DFT) study aimed at understanding structure–reactivity relationships in the oxidized metabolites of isomeric dibenzopyrenes (DBPs) and naphthopyrene (NP) is reported. These large polycyclic aromatic hydrocarbons (PAHs) contain a pyrene moiety and two benzannelated rings or a naphtho ring, and depending on the annelation mode, possess a fjord region (DB[*a*,*l*]P and N[1,2-*a*]P) or two or three bay-regions (DB[*a*,*h*]P, DB[*a*,*i*]P, and DB[*a*,*e*]P). Relative energies of the resulting carbocations were examined and compared, taking into account the available biological activity data on these compounds. Geometrical, electronic and conformational issues were considered. Charge-delocalization modes in the resulting carbocations were deduced by the changes in charges derived from natural population analysis (NPA). The reported biological activity of these toxic PAHs was found to correlate with the degree of deviation from planarity of the aromatic system, in accord with the higher bioactivity of the fjord- and methylated bay-region compounds. On the other hand, relative formation of the possible carbocations derived from each PAH, as well as the activity order for compounds presenting similar distortions, were explained by their relative carbocation stabilities. The covalent adducts formed via the fjord-region diol epoxide of DB[*a*,*l*]P and the exocyclic amino group and the N-7 of guanine were computed, and relative energies and geometries of the resulting adducts were examined. Furthermore, PAH-purine base adduct formation was modeled inside a DNA fragment by means of the ONIOM method.

Introduction

Polycyclic aromatic hydrocarbons (PAHs) are widespread environmental pollutants that are well known as mutagenic/carcinogenic agents.[1] In order to exert their biological activity they must undergo metabolic activation by epoxidation and hydrolysis to form dihydrodiols, which are further epoxidized to form the electrophilic bay-region diol epoxides (DEs) (see Figure 1).[2] In the case of the extensively studied benzo[*a*]pyrene (BaP) metabolites, among the four possible isomeric bay-region DEs (series-2: ± *anti* and series-1: ± *syn*), only a single *anti* isomer possesses strong tumorigenic activity, whereas the other enantiomer is moderately active, and the series-1 pair (*syn*) are inactive.[3]

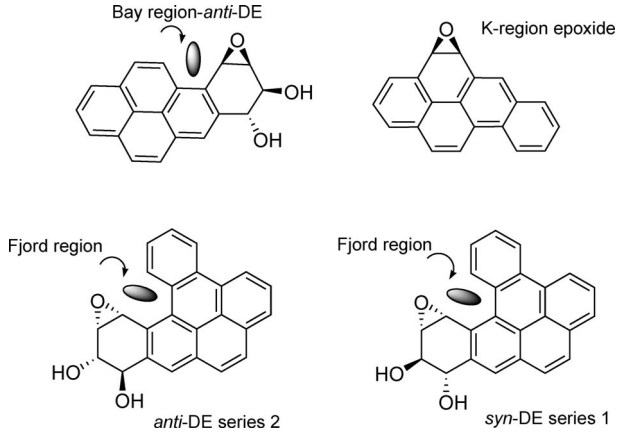

Figure 1. Bay-region *anti*-DE of BaP, K-region epoxide of BaP, and *anti*- and *syn*-DEs of DB[*a*,*l*]P as representative oxidized metabolites.

Opening of the *O*-protonated bay-region or K-region epoxide generates a benzylic carbocation, which is capable of forming covalent adducts with the nucleic acids.[2] In this way, a key step in the mechanism by which PAHs can alter the genetic material is through adduct formation, by reaction with the nucleophilic sites in DNA and RNA.[2]

[a] Unidad de Matemática y Física, INFIQC, Facultad de Ciencias Químicas, Universidad Nacional de Córdoba, Ciudad Universitaria,
Córdoba 5000, Argentina
Fax: +54-351-4344971
E-mail: gborosky@fcq.unc.edu.ar
[b] Department of Chemistry, Kent State University,
Kent, Ohio 44242, USA
Fax: +1-330-6723816
E-mail: klaali@kent.edu
Supporting information for this article is available on the WWW under http://dx.doi.org/10.1002/ejoc.200900xxx.

The DEs derived from PAHs that possess a fjord-region have been shown to be more potent carcinogens than those derived from bay-region PAHs (Figure 1).[4] The strong steric interactions in the fjord-region force the molecule to distort from planarity, and fjord-region modified-DNA adducts have been found to be more difficult to repair than the bay-region adducts.[5]

The fjord-region carcinogen dibenzo[*a*,*l*]pyrene (DB[*a*,*l*]P, **1**) (see Figure 2) was found to be significantly more potent than 7,12-dimethylbenzo[*a*]anthracene (7,12-DMBA, **2**) and benzo[*a*]pyrene (BaP, **3**), and it is considered to be the most toxic carcinogen among PAHs.[6]

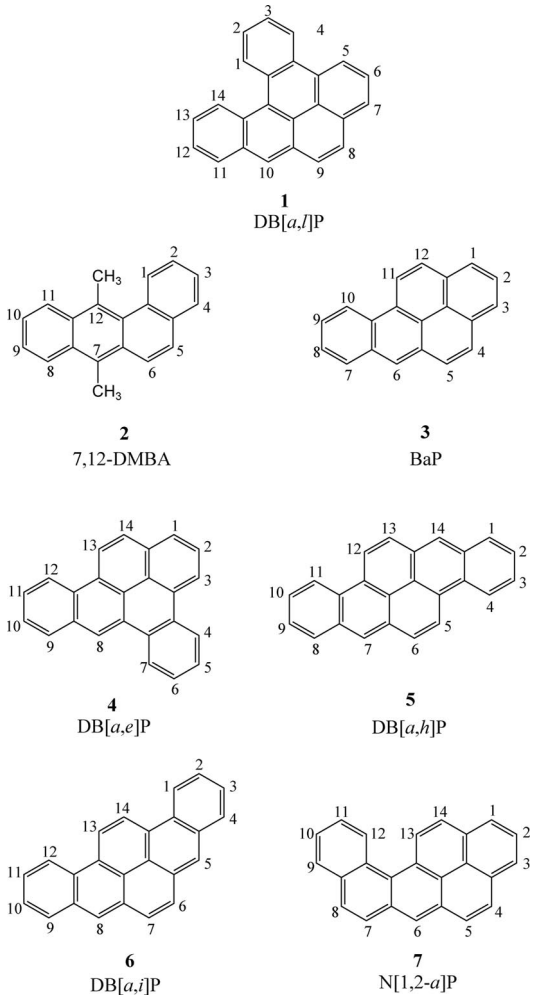

Figure 2. Isomeric dibenzopyrenes **1**, **4**, **5**, and **6** and naphthopyrene **7** together with **2** and **3**.

It was shown that enzymatic activation of DB[*a*,*l*]P leading to tumor initiation occurs by two main pathways: one-electron oxidation to yield radical cations,[7] and formation of fjord-region DB[*a*,*l*]*P*-11,12-dihydrodiol 13,14-epoxides.[8] Identification of DNA adducts revealed that both *syn*- and *anti*-DB[*a*,*l*]PDE are produced, and that DB[*a*,*l*]P is stereoselectively converted to (+)-*syn*- and (–)-*anti*-DB[*a*,*l*]PDE with 11*S*,12*R*,13*S*,14*R*- and 11*R*,12*S*,13*S*,14*R*-configurations, respectively.[8a,8c] In this case, the s*yn*-DB[*a*,*l*]PDE was found to be a more potent carcinogen than the corresponding *anti* diastereomer.[9]

Other hexacyclic PAHs containing a pyrene moiety possessing a fjord- and/or bay-region(s) are dibenzo[a,e]pyrene (DB[*a*,*e*]P, **4**), dibenzo[*a*,*h*]pyrene (DB[*a*,*h*]P, **5**), and dibenzo[*a*,*i*]pyrene (DB[*a*,*i*]P, **6**). Whereas **4** is mildly carcinogenic, **5** and **6** are both highly active, with **6** reported to be one of the most powerful sarcomagenic agents known (Figure 2).[10] However, they are much less potent than DB[*a*,*l*]P.[11,6b] Although DB[*a*,*h*]P and DB[*a*,*i*]P are potent tumorigens, they were less active than DB[*a*,*l*]P and BaP,[11,12] while DB[*a*,*e*]P was the least active compound in the series.[6b,12] Naphtho[1,2-*a*]pyrene (N[1,2-*a*]P, dibenzo-[*c*,*mno*]chrysene, **7**), another structural isomer of DB[*a*,*l*]P that presents a fjord-region, was found to have activity similar to that of BaP.[13]

Quantum-mechanical calculations, when applied to the study of the carcinogenic pathways of these compounds and the chemical reactivity of their ultimate carcinogenic metabolites, have shown very good agreement with the experimental bio-activities of several PAH (epoxides and DEs from BA, BaP, and BeP, as well as various amine, amide, episulfide and imine derivatives) and hetero-PAH metabolites (aza- and thia-PAHs).[14] Additionally, modeling studies on biological electrophiles from PAHs by density functional theory (DFT) methods have yielded appropriate descriptions of the NMR features and charge delocalization modes in the resulting delocalized carbocations.[15]

In the present work, we have performed a model DFT study on the structural and electronic properties of the electrophilic reactive intermediates of DB[*a*,*l*]P, DB[*a*,*e*]P, DB[*a*,*h*]P, DB[*a*,*i*]P, and N[1,2-*a*]P derivatives, for which changes in energy for epoxide ring-opening reactions were calculated. Comparisons were made with similar reactions for BaP and 7,12-DMBA. Conformational features and their relationship to reactivity were examined. Charge-delocalization modes (positive charge-density distribution) in the resulting carbocations were evaluated by means of the NPA (natural population analysis) derived changes in charges (carbocation minus neutral).

In our previous studies,[14a–14g] consideration of the solvent effect by means of polarized continuum-model (PCM) calculations did not afford significant variations in comparison to gas-phase reactivity trends. Whereas the reaction energies were certainly influenced by solvation, the reactivity orders and relatives stabilities for a series of compounds (epoxides, diol epoxides, and their derived carbocations) remained unchanged. Because the goal of the present study was to determine relative reactivities rather than to compute absolute reaction rates, gas-phase calculations were mostly carried out as a way to reduce the computational costs.

To model the crucial step of covalent adduct formation, adducts resulting from quenching of DB[*a*,*l*]PDE with guanine via the N-7 and the exocyclic amino group were computed in the gas phase and in dimethylformamide (DMF) as solvent, and their geometrical features and relative ener-

gies were compared. The choice of DMF as solvent for calculations was to mimic the previous experimental studies, in which the deoxyguanosine adducts were synthesized in DMF.[16]

In order to obtain a better estimation of the relevant adduct formation process in a more realistic model, covalent bond formation in PAH/purine was studied within the structure of a DNA fragment. This task was performed by combining DFT and semiempirical levels of theory employing the ONIOM method (see computational protocols section for details).

Results and Discussion

Changes in energy for the epoxide ring-opening reactions of several *O*-protonated dihydro-epoxide derivatives from **1**, **4**–**7** were calculated [Equation (1)]. Different bay- and fjord-region isomeric epoxides were considered. The K-region epoxides were also taken into account. The results are summarized in Table 1. The protonated epoxides, that is, the oxonium ions, could not be located as minima on the respective potential-energy surfaces, because epoxide ring opening ensued by a barrierless process upon *O*-protonation, this behavior was observed for every protonated epoxide in this study. In a previous work, calculations at the B3LYP/6-31+G** level gave rather similar results to those afforded by B3LYP/6-31G*.[14h] Therefore, the less computationally expensive 6-31G* basis set was employed in the present study.

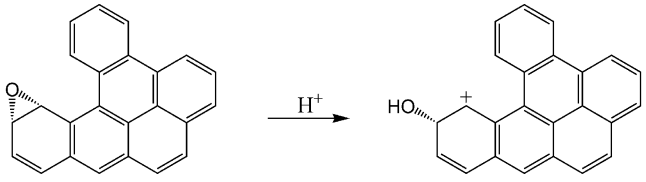

(1)

Table 1. Calculations of ring-opening reactions for epoxides (reaction 1).

Compound	Derivative	ΔE_r [kcal/mol]
DB[*a*,*l*]P (**1**)	1,2-epoxide	–241.48
	3,4-epoxide	–246.70
	13,14-epoxide	–243.64
DB[*a*,*e*]P (**4**)	4,5-epoxide	–241.67
	6,7-epoxide	–240.33
	11,12-epoxide	–244.65
DB[*a*,*h*]P (**5**)	2,3-epoxide	–268.50[a]
	3,4-epoxide	–247.31
	5,6-epoxide	–243.06
DB[*a*,*i*]P (**6**)	1,2-epoxide	–248.79
	6,7-epoxide	–233.31
N[1,2-*a*]P (**7**)	4,5-epoxide	–234.74
	7,8-epoxide	–237.59
	11,12-epoxide	–243.11

[a] A bay-region carbocation is generated.

Based on the data in Table 1, it is observed that opening of the *O*-protonated bay- and fjord-region epoxides is more favorable than opening of the K-region epoxides. These findings are in accordance with the higher toxicity of the fjord- and bay-region compounds.[2,4]

In the case of **5** (see Figure 2), opening of the K-region DB[*a*,*h*]P 2,3-epoxide generated the bay-region carbocation, with the cationic centre at C-4, which by the symmetry of the molecule, is equivalent to the C-11 carbocation. In this way, a relatively more stable bay-region carbocation was produced by protonation of a K-region epoxide due to electronic and geometrical reorganization; this fact causing the energetically most favorable ring opening reaction in Table 1.

Subsequently, calculations of the Equation 1 type were performed for all of the possible bay- and fjord-region DEs that could be formed from **1**, and **4**–**7**. Both *anti*- and *syn*-isomeric DEs were considered for each compound (only for the preferred opening reaction mode of DB[*a*,*l*]P and DB[*a*,*e*]P). Comparisons were made with the ΔE_r values obtained for BaP and 7,12-DMBA. The results are summarized in Table 2.

Table 2. Calculations of ring-opening reactions for DEs (reaction 1).

Compound	Derivative		ΔE_r [kcal/mol]
DB[*a*,*l*]P (**1**)	3,4-diol 1,2-epoxide		–241.91
	1,2-diol 3,4-epoxide		–241.44
	11,12-diol 13,14-epoxide	*anti*	–243.09 (–0.067)[a]
		syn	–246.82
DB[*a*,*e*]P (**4**)	6,7-diol 4,5-epoxide		–238.78
	4,5-diol 6,7-epoxide		–238.05
	9,10-diol 11,12-epoxide	*anti*	–242.37 (–0.126)[a]
		syn	–249.76
DB[*a*,*h*]P (**5**)	1,2-diol 3,4-epoxide	*anti*	–245.46 (–0.065)[a]
		syn	–249.29
DB[*a*,*i*]P (**6**)	3,4-diol 1,2-epoxide	*anti*	–247.14 (–0.083)[a]
		syn	–253.97
N[1,2-*a*]P (**7**)	9,10-diol 11,12-epoxide	*anti*	–239.74 (–0.041)[a]
		syn	–242.16
7,12-DMBA (**2**)	3,4-diol 1,2-epoxide	*anti*	–246.64 (–0.130)[a]
		syn	–245.54
BaP (**3**)	7,8-diol 9,10-epoxide	*anti*	–241.03 (–0.117)[a]
		syn	–246.96

[a] Change of NPA charge at the carbocationic center (carbocation minus neutral epoxide).

DB[*a*,*l*]P **1** has been found to be metabolically activated almost exclusively at the fjord-region to produce DB[*a*,*l*]*P*-11,12-diol 13,14-epoxide.[17] Accordingly, the data in Table 2 predict that this derivative is the one that generates the most stable carbocation from the parent compound. For both *anti*- and *syn*-isomers the conformation of the hydroxy groups was preferentially pseudodiequatorial, in accord with the reported NMR studies.[18] In addition, DB[*a*,*h*]P was found to be metabolized only at the bay-region benzo rings *a* and *h* (which are equivalent), while the K-region (C-5, C-6) was not involved in the formation of reactive intermediates that were bound to DNA.[19] Therefore, the agreement between the present calculations and the known bioactivity of these compounds is noteworthy.

The general trend of more favorable ΔE_rs for the *syn*-DEs observed in this work can be attributed to the fact that

the *anti*-DEs are more stable than their *syn*-isomers. The *anti*-disposition permits a stronger hydrogen-bond interaction between the oxygen atom of the epoxide and the hydrogen of the vicinal hydroxy group [O–H distance of 2.9 Å (atoms on the same side of the ring) vs. 3.6 Å for the *syn* DE (atoms on opposite sides of the ring)]. In this model, the opening of the *syn*-fjord region DB[*a*,*l*]PDE is preferred, in accord with the higher carcinogenicity that had been reported for this diastereomer.[9] However, the most tumorigenic metabolite of BaP is the *anti*-7,8-diol 9,10-epoxide-2 diastereomer,[3] which is in contrast with the relative ΔE_r values displayed in Table 2 for their *syn*- and *anti*-isomeric DEs. Nevertheless, it should be taken into account that relative bioactivities could be affected by alignment with the DNA helix and the intercalation issues, which were not considered in these calculations.

For stereoisomeric (+)-*syn*- and (–)-*anti*-DB[*a*,*l*]*P*-11,12-dihydrodiol 13,14-epoxide, more detailed calculations were performed, considering the different conformers of the epoxide and the open carbocation, with the hydroxy groups in pseudodiequatorial or in pseudodiaxial position (Table 3). The pseudodiequatorial conformation was preferred in all cases, as this arrangement allowed stronger hydrogen-bond interactions between the hydroxy groups. The epoxides exhibited a twisted half-boat structure, while the carbocations presented a twisted half-chair conformation. It should be noted that the lowest energy conformation for every diol epoxide and carbocation in this study was the one with the hydroxy groups in pseudodiequatorial disposition, in accordance with the available experimental results,[8b,18] and with a recent report on BaP-DEs.[20] The present calculations are in general agreement with previous lower level computational studies on DB[*a*,*l*]PDEs[21] and other fjord-region DEs[22] regarding the three-dimensional structures and relative stabilities of the different possible conformations.

Table 3. Calculations for DB[*a*,*l*]*P*-11,12-dihydrodiol 13,14-epoxide.

11,12-Diol conformation	Epoxide	Open carbocation	ΔE_r [kcal/mol]
DE-2 (*anti*)			
pseudoequatorial	twisted half-boat	twisted half-chair	–243.09
pseudoaxial	twisted half-boat	twisted half-chair	–242.74
DE-1 (*syn*)			
pseudoequatorial	twisted half-boat	twisted half-chair	–246.82
pseudoaxial	twisted half-boat	twisted half-chair	–251.18

Charge delocalization modes (positive charge density distribution) in the resulting carbocations were evaluated by means of the NPA-derived changes in charges for the carbon atoms (carbocation minus neutral). Charge delocalization maps for the *anti*-DEs are shown in Figure 3, where a threshold value of 0.030 was considered for C Δcharges. According to these NPA-derived charge distributions, positive charge in the resulting carbocations was delocalized throughout the π-system. Thus, the degree of delocalization of the net positive charge within the aromatic system was indicated by the development of negative charge density at the carbocationic center. In this way, the carbocation derived from N[1,2-*a*]P (**12**) was the least delocalized. However, no clear correlation with relative biological activities was found for the computed ΔE_r values (Table 2), which reflect relative carbocation stabilities, and/or negative charge densities at the carbocationic centers (Figure 3).

However, inspection of the geometries of the DEs and the derived carbocations revealed that the most stable carbocations were those whose aromatic systems deviated the least from planarity, because of a stronger resonance effect (Figure 4). Furthermore, correlation was observed between the relative activities of the studied PAHs and the distortion of the corresponding aromatic systems. In this way, ΔE_r values for the most deviated (and active) DEs **13**–**15** did not match with their higher activity, because destabilized strained epoxides are more prone to ring opening upon protonation, even though their derived carbocations are less stable than those derived from the more planar PAHs **16**, **18**, **19**. Hence, the relative activity of this family of isomeric PAHs seems to be primarily influenced by the effects of distortion of the DEs. Therefore, deviation from planarity appears to be the main determining factor of activity in the DEs, in comparing different PAHs. This finding explains the higher activity of the fjord-region and the methylated bay-region PAHs as compared to the bay-region analogs.

Conversely, stability determines the relative capability for the formation of diverse carbocations that can be derived from a given structure. In this way, the present ΔE_rs reasonably agree with the preferential metabolic activation at the fjord- or bay-region that have been experimentally observed for these compounds, instead of K-region activation. The relative stability principle also applies when analysing the relative activity of isomeric compounds which present similar distortion of the aromatic system **4**–**6**, although the higher activity of **3** over **4**–**6** could not be explained by this assumption. Nevertheless, **3** has one less fused aromatic ring than isomeric **4**–**6**, and this could be the reason for lower relative stability calculated for its carbocation.

Identification and quantification of DNA adducts of DB[*a*,*l*]P and its metabolites in vitro and in vivo have been reported.[9b,9c] Isolation and characterization of the adducts formed by stereoisomeric (±)-*syn* and (±)-*anti*-DB[*a*,*l*]*P*-11,12-dihydrodiol 13,14-epoxides with deoxyguanosine in DMF have also been described.[16] In the present work, the *trans* and *cis* adducts of (+)-*syn*- and (–)-*anti*-DB[*a*,*l*]PDE with guanine were computed, in order to examine their structures and relative energies. The covalent adducts formed by nucleophilic addition via the exocyclic amino group and the N-7 of guanine were considered. Conformational searches were performed by rotation of the generated C–N bond employing the AM1 semiempirical method, in order to find the most stable conformer for each adduct. These lowest energy structures were subsequently optimized by DFT calculations. Geometry optimizations were carried out both in gas phase and in DMF as solvent (by PCM method; see computational details).

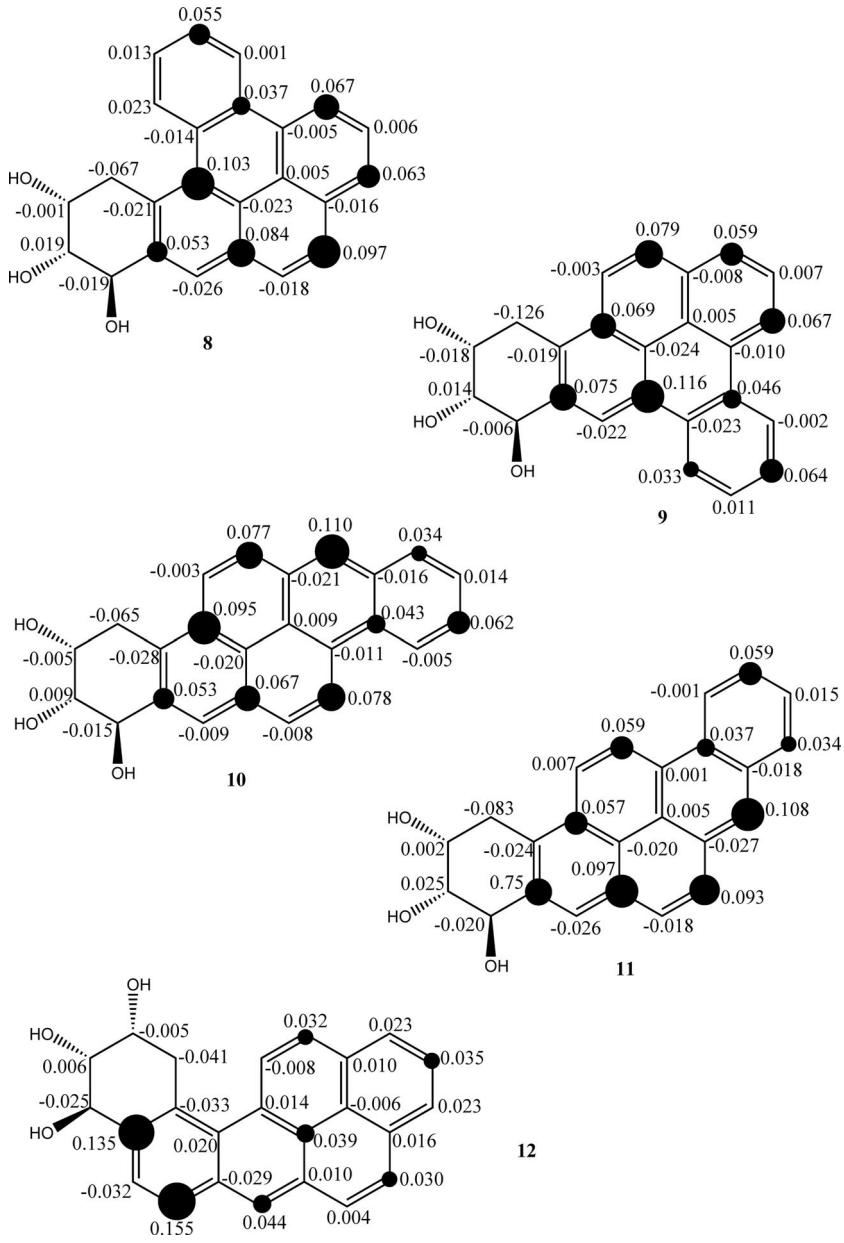

Figure 3. Computed NPA carbon atom changes in charge densities for the carbocations generated from *anti*-DEs (the dark circles are roughly proportional to the magnitude of C Δcharges; threshold was set to 0.030).

In the gas phase, the most stable adduct was the *syn-cis*-DB[*a*,*l*]PDE-N^{2}Gua, formed by *cis*-opening of DB[*a*,*l*]PDE and covalent bond formation with the exocyclic nitrogen of guanine, followed in stability by the *anti-cis*-DB[*a*,*l*]PDE-N^{2}Gua adduct. In all cases, the cyclohexenyl ring preferred to adopt a twisted half-boat configuration. The hydroxy groups were either in pseudoequatorial or pseudoaxial conformation, depending on the compound. For the guanine moiety, the pseudoaxial disposition was preferred in most cases. Relative energies and conformational features of the covalent adducts are presented in Table 4, and selected structures are shown in Figure 5.

In DMF as solvent, there were some variations in relative energies of the different adducts, but no conformational changes were observed in comparison to the gas-phase structures. Differences in the computed relative energies in DMF vs. gas phase for the indicated structures are attributed to opposing trends observed between "cavity formation" within the solvent structure to include solute, and the electrostatic solute-solvent interaction energies.

The primary binding sites in DNA for the DB[*a*,*l*]PDEs under consideration are the exocyclic N^6-amino groups of deoxyadenosine and the corresponding N^2-amino groups of deoxyguanosine.[23] Reaction with the exocyclic amino groups of adenine or guanine leads to the formation of adducts that are stable under normal DNA isolation procedures,[8d,24] while binding to the N-3 or N-7 positions of adenine or the N-7 position of guanine leads to depurinated adducts.[7a] Treatment of mouse skin with these DB[*a*,*l*]-PDEs predominantly formed stable guanine adducts.[9c]

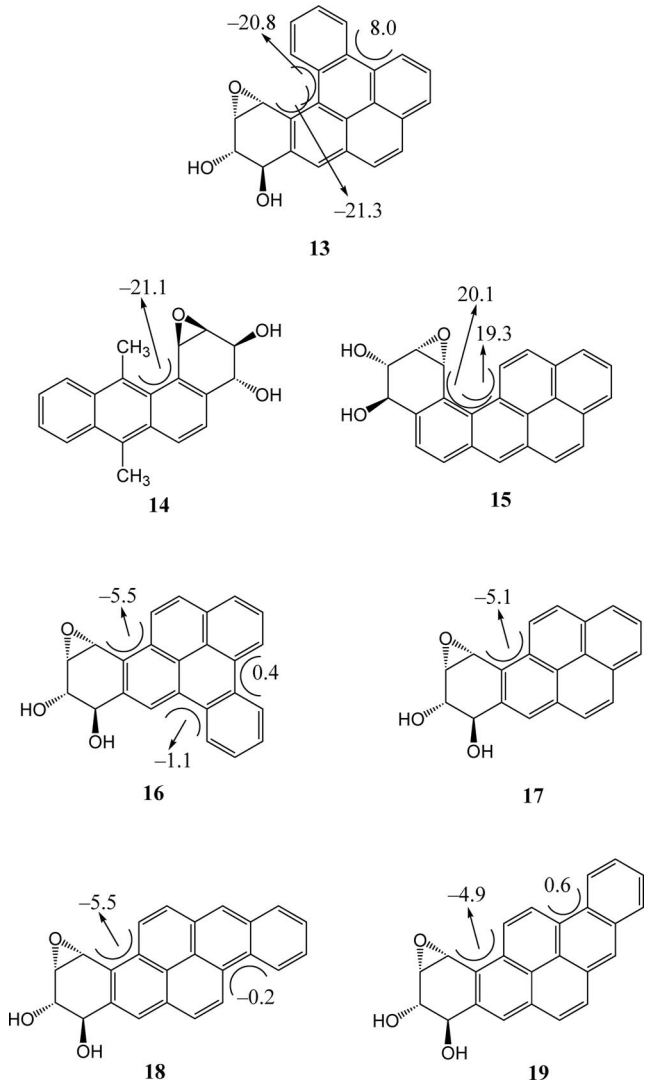

Figure 4. Dihedral angles (degree) showing the deviation from planarity of the ring system at fjord and bay regions for *anti*-DEs.

Theoretical results in the present work, indicating preferential reactivity with the exocyclic amino group, notably agree with the experimental observations reported in the literature.

With the aim of attaining a more realistic examination of the crucial PAH-DNA covalent adduct formation process, this reaction was also explored within the framework of a DNA fragment. Therefore, ONIOM (B3LYP/6-31+G*:PM3MM) calculations were carried out for adduct formed between *syn*-DB[*a*,*l*]PDE and the amino group of an adenine, in a DNA fragment consisting of five pairs of complementary bases with their corresponding sugar units and phosphate groups (Figure 6). The non-covalent intercalation complex between the carbocation derived from *syn*-DB[*a*,*l*]PDE and the DNA bases was also studied (Figure 6). Using this approach, the difference in energy between this precursor and that of the covalent adduct was taken as the reaction energy for adduct formation.

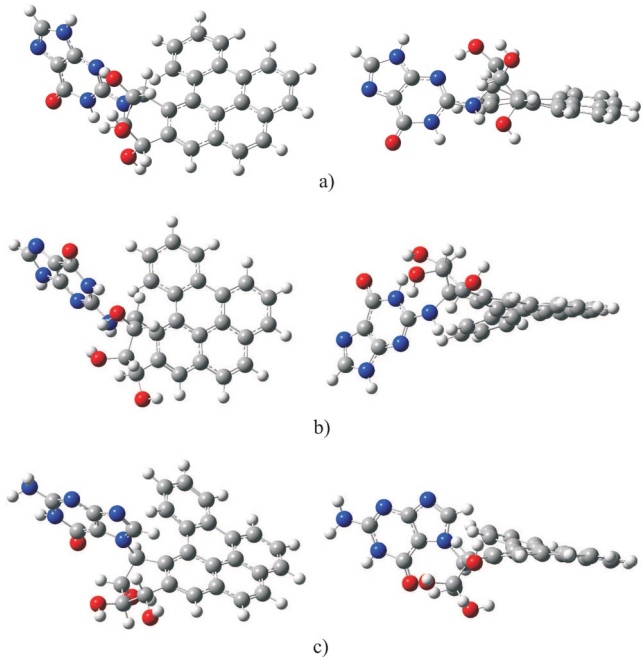

Figure 5. Lowest energy exocyclic and N-7 adducts of DB[*a*,*l*]*P*-11,12-diol 13,14-epoxide with guanine. (a) Exocyclic c*is-syn* adduct. (b) Exocyclic *cis-anti* adduct. (c) N-7 *trans-syn* adduct.

Intercalation of the PAH-DE did not significantly alter the hydrogen-bond pairing between the neighboring complementary bases (not involved in covalent binding). Instead, loss of hydrogen bonding between the reactive adenine and its complementary thymine was compensated by hydrogen bond interactions with the carbocation. Consequently, formation of the intercalation complex from the

Table 4. Calculations for guanine adducts of DB[*a*,*l*]*P*-11,12-dihydrodiol 13,14-epoxide.

Stereoisomeric adduct		Relative energy [kcal/mol][a]		Cyclohexenyl ring conformation	Conformation of substituents			
		gas phase	DMF		11-OH	12-OH	13-OH	14-Gua
exocyclic	*trans-anti*	4.6	4.6	twisted half-boat	pseudoaxial	pseudoequatorial	pseudoaxial	pseudoaxial
NH_2	*cis-anti*	1.5	0.1	twisted half-boat	pseudoequatorial	pseudoequatorial	pseudoequatorial	pseudoaxial
	trans-syn	7.7	2.8	twisted half-boat	pseudoequatorial	pseudoequatorial	pseudoequatorial	pseudoaxial
	cis-syn	0.0	0.0	twisted half-boat	pseudoaxial	pseudoequatorial	pseudoequatorial	pseudoaxial
N-7	*trans-anti*	0.4	4.2	twisted half-boat	pseudoaxial	pseudoequatorial	pseudoaxial	pseudoaxial
	cis-anti	1.5	0.2	twisted half-chair	pseudoequatorial	pseudoequatorial	pseudoaxial	pseudoequatorial
	trans-syn	0.0	0.0	twisted half-boat	pseudoequatorial	pseudoaxial	pseudoequatorial	pseudoaxial
	cis-syn	4.7	7.9	twisted half-boat	pseudoequatorial	pseudoaxial	pseudoaxial	pseudoequatorial

[a] Relative to the most stable structure in the gas phase and in DMF.

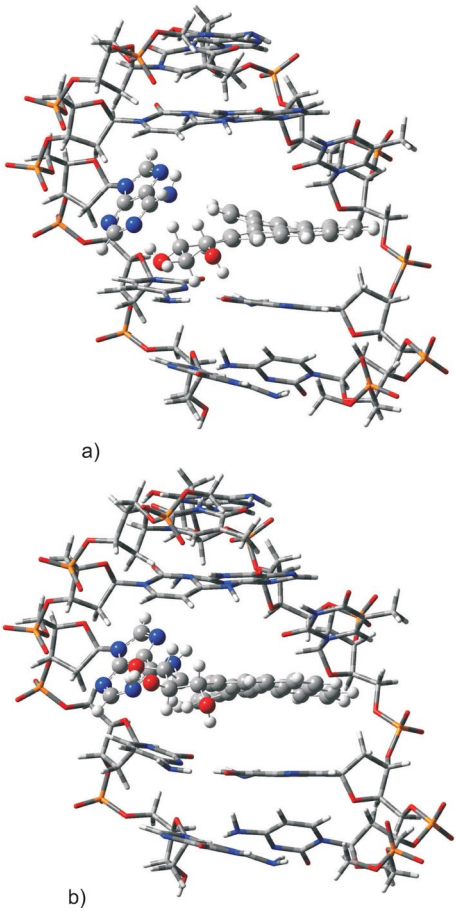

Figure 6. DNA fragment with DB[*a*,*l*]PDE. (a) Intercalation complex. (b) Covalent adduct.

separate components (DNA fragment plus *syn*-DB[*a*,*l*]-PDE) became exothermic.

For comparison purposes, the corresponding ONIOM calculations were also performed for the carbocation derived from *syn*-DB[*a*,*e*]PDE, the least biologically active compound in the series. DNA adduct formation was more favored for DB[*a*,*e*]PDE by ca. 17 kcal/mol, in contrast with the reported bioactivity data. Also, the intercalation complex with DB[*a*,*e*]PDE was relatively more stable by around 8 kcal/mol than the corresponding one for DB[*a*,*l*]PDE. The present results are in concert with the mechanistic studies on the hydrolysis of the BaP-DE, which proposed that a physically-bound DE reacts to form a physically bound benzylic carbocation in the rate-determining step.[25] Moreover, recent theoretical studies showed that the ΔE_r for reactions with nucleophiles, in the case of carbocations of phenanthrene derivatives and those derived from aza-PAHs, did not correlate with the known relative experimental activities of these compounds, suggesting that stability/lifetime of the PAH carbocations, formed by epoxide ring opening by an S_N1-like process, is the determining factor of their relative reactivity.[14d] Furthermore, previous studies have shown that the epoxidation step, calculated for different positions in several different PAHs, yielded almost the same energy change, and was considerably less exothermic relative to carbocation formation.[14h]

Concluding Remarks

The DFT calculations in the present model study focusing on the fjord- or bay-region diol epoxide metabolites of isomeric dibenzopyrenes **1**, **4**, **5**, and **6** and the naphthopyrene **7** appear to correlate with the available literature data on the biological activities of their DEs. For the distorted fjord-region PAHs, such as DB[*a*,*l*]P, calculations for DEs gave more consistent results with the measured bioactivities than computations for the corresponding epoxides. Therefore, the activity of this family of isomeric PAHs seems to be determined by the degree of deviation from planarity of the aromatic system. This fact accounts for the higher reactivity of the fjord- and methylated bay-region structures. On the other hand, among the possible carbocations that can be generated from a given PAH, the most stable one is formed. Relative carbocation stability also explains the activity order in similarly distorted isomeric structures.

For every DE and carbocation in this study, the lowest energy conformation was the one with the hydroxy groups in a pseudodiequatorial disposition, because this arrangement permits stronger hydrogen-bond interactions between the hydroxy groups. Computations determined that the *anti*-DEs are generally more stable than their *syn* isomers, because the *anti*-disposition permits a stronger hydrogen-bond interaction between the oxygen atom of the epoxide and the hydrogen of its vicinal hydroxy group.

ONIOM computations for adduct formation reactions, considering initial intercalation and positioning with respect to the DNA helix, reinforce the notion that the relative stability of the generated carbocations is an important determining factor for their mutagenic/carcinogenic activity.

Bioactivity of mutagens/carcinogens is brought about by complex processes involving a number of metabolic and chemical steps. Nevertheless, the present study indicates that DFT calculations can provide reasonable estimations of relative activity for structurally related compounds, with a moderate computational cost, encouraging their use as a predictive tool. More accurate relative reactivities of the ultimate carcinogens should comprise higher level simulations, as well as solvation effects.

In due course, synthesis, isolation and characterization of DNA adducts of isomeric DBPs, for which these data are still unavailable, will allow a more comprehensive evaluation of the binding modes, conformational features and preferred adducts that are predicted by the theoretical results in this work.

Experimental Section

Computational Details: DFT calculations were performed with the Gaussian 03 suite of programs,[26] using the B3LYP functional[27] and the 6-31G* split-valence shell basis set. Geometries were fully

optimized and minima were characterized by calculation of the harmonic vibrational frequencies. Natural bond orbital population analysis (NPA) was evaluated by means of the NBO program.[28] The effect of solvation in DMF was estimated by geometry optimizations with the polarized continuum model (PCM).[29] Because the Gaussian program does not provide an option for DMF as a solvent, computations were carried out for acetonitrile (AN) instead, which has nearly the same dielectric constant. Additionally, adjustable parameters in the PCM method were modified to fit the DMF values, and the energies obtained by this procedure differed from the AN results by less than 1 kcal/mol. Semiempirical calculations (preliminary conformational searches, not included) were carried out with the AM1 method.[30]

Three-dimensional coordinates of the DNA fragment were obtained from the Protein Data Bank (PDB code 1JDG).[31] The structure of the adduct adenine-*syn*-BaP-DE was utilized as a template in order to build the initial data for the DB[*a*,*l*]P and DB[*a*,*e*]-P adduct calculations. The employed DNA fragment consisted of five pairs of DNA complementary bases with their corresponding ten sugar units and ten phosphate groups, which were deprotonated. Calculations were performed using a two-layer ONIOM approach,[32] the high layer consisting of the DE and adenine (B3LYP/6-31+G* level), while for the rest of the system (low layer) the PM3MM semiempirical method was employed.[33] The DNA double-helix structure was retained by fixing the coordinates of the phosphate groups, and the sugar atoms to which they were linked, while the coordinates of all the other atoms were fully optimized.

Acknowledgments

This study was supported in part by the National Cancer Institute (NCI) of National Institutes of Health (NIH) (2R15-CA078235-02A1). G. L. B gratefully acknowledges financial support from Consejo Nacional de Investigaciones Científicas y Técnicas (CONICET) and the Secretaría de Ciencia y Tecnología de la Universidad Nacional de Córdoba (Secyt-UNC).

[1] International Agency for Research on Cancer, *IARC Monographs on the Evaluation of the Carcinogenic Risks to Humans*, *vol. 32: Polycyclic Aromatic Compounds*, *Part 1*, *Chemical Environmental and Experimental Data*, IARC, Lyon, **1983**.

[2] R. G. Harvey, *Polycyclic Aromatic Hydrocarbons: Chemistry and Carcinogenicity*, Cambridge University Press, Cambridge, UK, **1991**.

[3] a) D. M. Jerina, H. Yagi, D. R. Thakker, J. M. Sayer, P. J. van Bladeren, R. E. Lehr, D. L. Whalen, W. Levin, R. L. Chang, A. W. Wood, A. H. Conney, in: *Foreign Compound Metabolism* (Eds.: J. Caldwell, G. D. Paulson), Taylor and Francis, LTF, London, **1984**, pp. 257–266; b) A. H. Conney, *Cancer Res.* **1982**, *42*, 4875–4917.

[4] a) S. Amin, J. Krzeminski, A. Rivenson, C. Kurtzke, S. S. Hecht, K. El-Bayoumy, *Carcinogenesis* **1995**, *16*, 1971–1974; b) S. S. Hecht, K. El-Bayoumy, A. Rivenson, S. Amin, *Cancer Res.* **1994**, *54*, 21–24; c) W. Levin, A. W. Wood, R. L. Chang, Y. Ittah, M. Croisy-Delcey, H. Yagi, D. M. Jerina, A. H. Conney, *Cancer Res.* **1980**, *40*, 3910–3914; d) S. Amin, D. Desai, W. Dai, R. G. Harvey, S. S. Hecht, *Carcinogenesis* **1995**, *16*, 2813–2817.

[5] a) K. Dreij, A. Seidel, B. Jernstrom, *Chem. Res. Toxicol.* **2005**, *18*, 655–664; b) T. Buterin, T. M. Hess, N. Luneva, N. E. Geacintov, S. Amin, H. Kroth, A. Seidel, H. Naegeli, *Cancer Res.* **2000**, *60*, 1849–1856; c) D. R. Lloyd, P. C. Hanawalt, *Cancer Res.* **2002**, *62*, 5288–5294; d) D. R. Lloyd, P. C. Hanawalt, *Cancer Res.* **2000**, *60*, 517–521.

[6] a) E. L. Cavalieri, S. Higginbotham, N. V. RamaKrishna, P. D. Devanesan, R. Todorovic, E. G. Rogan, S. Salmasi, *Carcinogenesis* **1991**, *12*, 1939–1944; b) E. L. Cavalieri, E. G. Rogan, S. Higginbotham, P. Cremonesi, S. Salmasi, *J. Cancer Res. Clin. Oncol.* **1989**, *115*, 67–72; c) S. Higginbotham, N. V. RamaKrishna, S. L. Johansson, E. G. Rogan, E. L. Cavalieri, *Carcinogenesis* **1993**, *14*, 875–878; d) A. K. Prahalad, J. A. Ross, G. B. Nelson, B. C. Roop, L. C. King, S. Nesnow, M. J. Mass, *Carcinogenesis* **1997**, *18*, 1955–1963; e) J. Schwartz, V. Baker, E. Larios, D. Desai, S. Amin, *Oral Oncol.* **2004**, *40*, 611–623; f) D. Xu, Y. Duan, I. A. Blair, T. M. Penning, R. G. Harvey, *Org. Lett.* **2008**, *10*, 1059–1062.

[7] a) K.-M. Li, R. Todorovic, E. G. Rogan, E. L. Cavalieri, F. Ariese, M. Suh, R. Jankowiak, G. J. Small, *Biochemistry* **1995**, *34*, 8043–8049; b) E. L. Cavalieri, E.G. Rogan, in *The Handbook of Environmental Chemistry, vol. 3, part I, PAHs and Related Compounds* (Ed.: A. H. Neilson), Springer-Verlag, Berlin, Heidelberg, Germany, **1998**; c) R. Jankowiak, G. J. Small, in *The Handbook of Environmental Chemistry, vol. 3, part I, PAHs and Related Compounds* (Ed.: A. H. Neilson) Springer-Verlag, Berlin, Heidelberg, Germany, **1998**.

[8] a) S. L. Ralston, A. Seidel, A. Luch, K. L. Platt, W. M. Baird, *Carcinogenesis* **1995**, *16*, 2899–2907; b) A. Luch, H. Glatt, K. L. Platt, F. Oesch, A. Seidel, *Carcinogenesis* **1994**, *15*, 2507–2516; c) S. L. Ralston, H. H. S. Lau, A. Seidel, A. Luch, K. L. Platt, W. M. Baird, *Cancer Res.* **1994**, *54*, 887–890; d) K.-M. Li, N. V. S. RamaKrishna, N. S. Padmavathi, E. G. Rogan, E. L. Cavalieri, *Polycyclic Aromat. Compd.* **1994**, *6*, 207–213.

[9] a) H. S. Gill, P. L. Kole, J. C. Wiley, K.-M. Li, S. Higginbotham, E. G. Rogan, E. L. Cavalieri, *Carcinogenesis* **1994**, *15*, 2455–2460; b) E. L. Cavalieri, E. G. Rogan, K.-M. Li, R. Todorovic, F. Ariese, R. Jankowiak, N. Grubor, G. J. Small, *Chem. Res. Toxicol.* **2005**, *18*, 976–983; c) R. Todorovic, P. Devanesan, E. Rogan, E. Cavalieri, *Chem. Res. Toxicol.* **2005**, *18*, 984–990.

[10] J. F. Waterfall, P. Sims, *Biochem. Pharmacol.* **1973**, *22*, 2469–2483.

[11] W. F. Busby Jr., H. Smith, C. L. Crespi, B. W. Penman, *Mutat. Res.* **1995**, *342*, 9–16.

[12] N. C. Hughes, D. H. Phillips, *Carcinogenesis* **1990**, *11*, 1611–1619.

[13] a) G. Nelson, J. A. Ross, M. Pimentel, D. Desai, A. K. Sharma, S. Amin, S. Nesnow, *Cancer Lett.* **2007**, *247*, 309–317; b) D. Desai, A. K. Sharma, J.-M. Lin, J. Krzeminski, M. Pimentel, K. El-Bayoumy, S. Nesnow, S. Amin, *Chem. Res. Toxicol.* **2002**, *15*, 964–971.

[14] a) G. L. Borosky, *J. Org. Chem.* **1999**, *64*, 7738–7744; b) G. L. Borosky, *Helv. Chim. Acta* **2001**, *84*, 3588–3599; c) G. L. Borosky, *J. Comput. Chem.* **2003**, *24*, 601–608; d) G. L. Borosky, K. K. Laali, *Org. Biomol. Chem.* **2005**, *3*, 1180–1188; e) G. L. Borosky, K. K. Laali, *Chem. Res. Toxicol.* **2005**, *18*, 1876–1886; f) G. L. Borosky, K. K. Laali, *Chem. Res. Toxicol.* **2006**, *19*, 899–907; g) G. L. Borosky, *Chem. Res. Toxicol.* **2007**, *20*, 171–180; h) G. L. Borosky, K. K. Laali, *Org. Biomol. Chem.* **2007**, *5*, 2234–2242; i) K. K. Laali, J.-H. Chun, T. Okazaki, S. Kumar, G. L. Borosky, C. Swartz, *J. Org. Chem.* **2007**, *72*, 8383–8393; j) G. L. Borosky, *J. Mol. Graphics Modell.* **2008**, *27*, 459–465.

[15] a) T. Okazaki, K. K. Laali, B. Zajc, M. K. Lakshman, S. Kumar, W. M. Baird, W.-M. Dashwood, *Org. Biomol. Chem.* **2003**, *1*, 1509–1516; b) K. K. Laali, T. Okazaki, S. Kumar, S. E. Galembeck, *J. Org. Chem.* **2001**, *66*, 780–788; c) K. K. Laali, in *Carbocation Chemistry* (Eds.: G. A. Olah, G. K. S. Prakash), Wiley, **2004**, chapter 9; d) T. Okazaki, K. K. Laali, *Org. Biomol. Chem.* **2003**, *1*, 3078–3093; e) T. Okazaki, K. K. Laali, *J. Org. Chem.* **2004**, *69*, 510–516.

[16] K.-M. Li, M. George, M. L. Gross, C.-H. Lin, R. Jankowiak, G. J. Small, A. Seidel, H. Kroth, E. G. Rogan, E. L. Cavalieri, *Chem. Res. Toxicol.* **1999**, *12*, 778–788.

[17] A. Luch, S. L. Coffing, Y. M. Tang, A. Schneider, V. Soballa, H. Greim, C. R. Jefcoate, A. Seidel, W. F. Greenlee, W. M. Baird, J. Doehmer, *Chem. Res. Toxicol.* **1998**, *11*, 686–695.

[18] J. Krzeminski, J.-M. Lin, S. Amin, S. S. Hecht, *Chem. Res. Toxicol.* **1994**, *7*, 125–129.

[19] G. A. Marsch, R. Jankowiak, G. J. Small, N. C. Hughes, D. H. Phillips, *Chem. Res. Toxicol.* **1992**, *5*, 765–772.

[20] J. D. Kubicki, *Am. J. Sci.* **2005**, *305*, 621–644.

[21] K.-B. Cho, K. Dreij, B. Jernström, A. Gräslund, *Chem. Res. Toxicol.* **2003**, *16*, 590–597.

[22] a) L. Lewis-Bevan, S. B. Little, J. R. Rabinowitz, *Chem. Res. Toxicol.* **1995**, *8*, 499–505; b) J. R. Rabinowitz, S. B. Little, L. Lewis-Bevan, *Polycyclic Aromat. Compd.* **1996**, *11*, 237–244; c) S. B. Little, J. R. Rabinowitz, P. Wei, W. Yang, *Polycyclic Aromat. Compd.* **1999**, *14*, 53–61.

[23] H. Yagi, H. Frank, A. Seidel, D. M. Jerina, *Chem. Res. Toxicol.* **2008**, *21*, 2379–2392 and references cited therein.

[24] P. D. Devanesan, E. G. Rogan, E. L. Cavalieri, *Proc. Am. Assoc. Cancer Res.***1995**, *36*, 137.

[25] a) N. B. Islam, D. L. Whalen, H. Yagi, D. M. Jerina, *J. Am. Chem. Soc.* **1987**, *109*, 2108–2111; b) S. C. Gupta, N. B. Islam, D. L. Whalen, H. Yagi, D. M. Jerina, *J. Org. Chem.* **1987**, *52*, 3812–3815.

[26] M. J. Frisch, G. W. Trucks, H. B. Schlegel, G. E. Scuseria, M. A. Robb, J. R. Cheeseman, J. A. Montgomery Jr., T. Vreven, K. N. Kudin, J. C. Burant, J. M. Millam, S. S. Iyengar, J. Tomasi, V. Barone, B. Mennucci, M. Cossi, G. Scalmani, N. Rega, G. A. Petersson, H. Nakatsuji, M. Hada, M. Ehara, K. Toyota, R. Fukuda, J. Hasegawa, M. Ishida, Y. Nakajima, O. Honda, O. Kitao, H. Nakai, M. Klene, X. Li, J. E. Knox, H. P. Hratchian, J. B. Cross, C. Adamo, J. Jaramillo, R. Gomperts, R. E. Stratmann, O. Yasyev, A. J. Austin, R. Cammi, C. Pomelli, J. W. Ochterski, P. Y. Ayala, K. Morokuma, G. A. Voth, P. Salvador, J. J. Dannemberg, V. G. Zakrzewski, S. Dapprich, A. D. Daniels, M. C. Strain, O. Farkas, D. K. Malick, A. D. Rabuck, K. Raghavachari, J. B. Foresman, J. V. Ortiz, Q. Cui, A. G. Baboul, S. Clifford, J. Cioslowski, B. B. Stefanov, G. Liu, A. Liashenko, P Piskorz, I. Komaromi, R. L. Martin, D. J. Fox, T. A. Keith, M. A. Al-Laham, C. Y. Peng, A. Nanayakkara, M. Challacombe, P. M. W. Gill, B. Johnson, W. Chen, M. W. Wong, C. Gonzalez, J. A. Pople, *Gaussian 03*, Revision B.05, Gaussian, Inc., Wallingford, CT, **2003**.

[27] a) A. D. Becke, *J. Chem. Phys.* **1993**, *98*, 5648–5652; b) C. Lee, W. Yang, R. G. Parr, *Phys. Rev. B* **1988**, *37*, 785–789; c) B. Miehlich, A. Savin, H. Stoll, H. Preuss, *Chem. Phys. Lett.* **1989**, *157*, 200–206.

[28] E. D. Glendening, A. E. Reed, J. E. Carpenter, F. Weinhold, *NBO Version 3.1*, Gaussian, Inc.: Wallingford, CT, **2003**.

[29] a) S. Miertus, E. Scrocco, J. Tomasi, *Chem. Phys.* **1981**, *55*, 117; b) M. T. Cances, V. Mennucci, J. Tomasi, *J. Chem. Phys.* **1997**, *107*, 3032; c) V. Barone, M. Cossi, J. Tomasi, *J. Comput. Chem.* **1998**, *19*, 404.

[30] M. J. S. Dewar, E. G. Zoebisch, E. F. Healy, J. J. P. Stewart, *J. Am. Chem. Soc.* **1985**, *107*, 3902–3909.

[31] P. Pradhan, S. Tirumala, X. Liu, J. M. Sayer, D. M. Jerina, H. J. C. Yeh, *Biochemistry* **2001**, *40*, 5870.

[32] S. Dapprich, I. Komáromi, K. S. Byun, K. Morokuma, M. J. Frisch, *THEOCHEM* **1999**, *462*, 1–21.

[33] J. J. P. Stewart, *J. Comput. Chem.* **1989**, *10*, 209.

Received: March 11, 2009
Published Online: May 21, 2009

